Tetrahedron 67 (2011) 9129–9133

Contents lists available at SciVerse ScienceDirect

Tetrahedron

journal homepage: www.elsevier.com/locate/tet

Conformation and stereodynamics of 1,2-diaryltetrahydropyrimidine and of its five- and seven-membered ring analogs

Jimena E. Díaz [b], Nadia Gruber [b], Lodovico Lunazzi [a], Andrea Mazzanti [a,*], Liliana R. Orelli [b,*]

[a] Department of Organic Chemistry 'A.Mangini', University of Bologna, Viale Risorgimento 4, Bologna 40136, Italy
[b] Departamento de Química Orgánica, Facultad de Farmacia y Bioquímica, Universidad de Buenos Aires, CONICET, Junin 956, Buenos Aires 1113, Argentina

ARTICLE INFO

Article history:
Received 7 June 2011
Received in revised form 29 August 2011
Accepted 20 September 2011
Available online 28 September 2011

Keywords:
Nitrogen heterocycles
Conformational analysis
Axial chirality
Dynamic NMR
DFT calculations

ABSTRACT

The 1-(2-nitrophenyl)-2-(2-methylphenyl)-1,4,5,6-tetrahydropyrimidine and its five- and seven-membered ring analogs were synthesized and their conformational properties investigated by low temperature NMR spectroscopy and DFT theoretical calculations. Restricted rotation of the aryl substituents were observed in all cases and the corresponding barriers determined. In the case of the six-membered ring derivative the additional conformers resulting from a ring inversion process were also detected.

© 2011 Elsevier Ltd. All rights reserved.

1. Introduction

Tetrahydropyrimidines bearing a variety of substituents display biological and pharmacological properties[1–3] in that they can be used, for instance, as antidepressants,[4] fungicides,[5] and anthelmintics.[6] In the past we had investigated, by NMR spectroscopy, the conformational and stereodynamic properties of a number of diaryl derivatives of these compounds[7,8] that showed, at low temperature, the existence of conformational diastereoisomers due to the restricted rotation about the aryl-pyrimidinyl rings. In the present work we have investigated the behavior of analogous compounds having, in addition to the six-membered ring, also the smaller and the larger five- and seven-membered rings, respectively.

2. Results and discussion

For this purpose compounds **1**–**4** were synthesized.

The ^{1}H NMR spectroscopic signals (at 600 MHz in CDF_2Cl/$CDFCl_2$) of compound **1**, that are sharp at ambient temperature, broaden on cooling and split into two groups of lines of almost equal intensity below −100 °C. This effect is most clearly visible in the case of the methyl signal, which decoalesces below −90 °C,

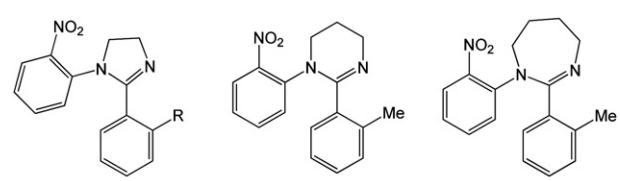

R= Me, **1**
R= H, **4**

2

3

yielding two sharp lines separated by 240 Hz at −130 °C with a 51:49 intensity ratio.[9] The rate constants of the process (k in s^{-1}), obtained at various temperatures by a line shape simulation (Fig. 1), afforded the free energy of activation $\Delta G^{\neq}$ by applying the Eyring equation (8.6 kcal/mol).[10] As usual for conformational processes, in this case and in all the cases investigated hereafter the activation energy $\Delta G^{\neq}$ was found to be virtually invariant in the observed temperature range, thus implying a very small (or negligible) activation entropy $\Delta S^{\neq}$.[11]

The observation of separate lines implies the existence of two conformers that were interpreted as due to the restricted rotation of both aryl groups. In fact, the conformation adopted is expected to have the aryl planes not coplanar with the averaged dynamic plane (due to the extremely rapid inversion) of the five-membered diaza ring: in this non-planar situation the NO_2 and Me groups can stay,

* Corresponding authors. E-mail address: andrea.mazzanti@unibo.it (A. Mazzanti).

0040-4020/$ – see front matter © 2011 Elsevier Ltd. All rights reserved.
doi:10.1016/j.tet.2011.09.091

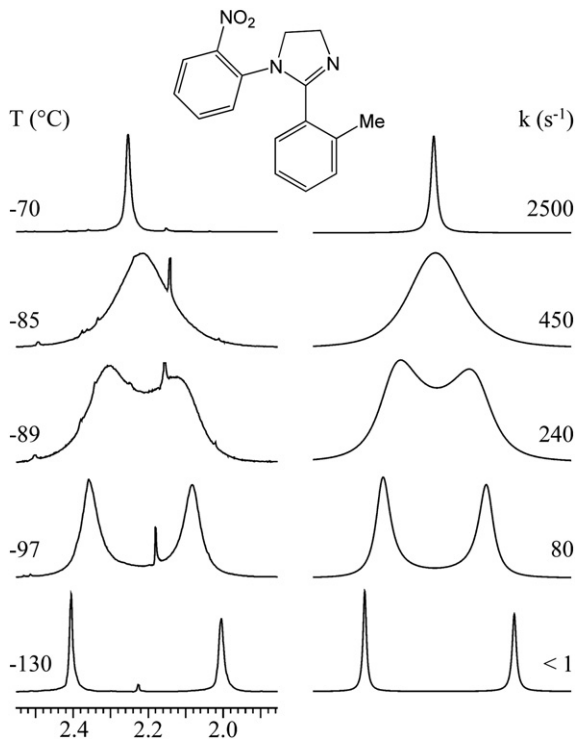

Fig. 1. Left: temperature dependence of the methyl signal of **1** (600 MHz in CDF_2Cl/$CDFCl_2$). Right: line shape simulation with the rate constants reported.

accordingly, either in a cis or in a trans relationship (Scheme 1) to each other.

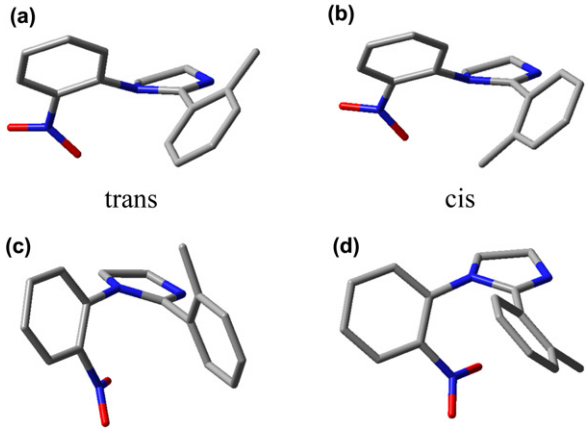

Scheme 1. DFT computed structures of the four ground state conformers of **1**.

In principle, the barriers for the rotation of the two aryl groups might be different, but such a difference is, apparently, too small to be appreciated experimentally. In fact, if the rotation of only one of the two rings had been locked at a given temperature (yielding a non-coplanar, thus chiral conformation) with the other ring still in rapid rotation, we should have observed diastereotopic methylene hydrogens (thus yielding anisochronous signals), whereas the methyl group should still display a single line. Only at a lower temperature, when also the rotation of the second ring would be frozen, the two methyl lines would separate, because only when both rings are locked the trans and cis conformers are generated. In contrast, the dynamic process was simultaneously detected by monitoring the methylene as well as the methyl signals, thus indicating that the rotation barriers of the two aromatic rings cannot be distinguished, within the experimental accuracy. The near identity of these two values is obviously the result of an accidental coincidence.

DFT calculations indicate the existence of four energy minima (Scheme 1), corresponding to a situation where the two rings adopt a twisted, thus chiral, conformation. The interconversion between the two cis (b,d), as well as that between the two trans (a,c), occurs via the so called π-barrier,[12] (i.e., the passage through an orthogonal transition state), with a value, which is exceedingly low for the dynamic NMR technique, thus experimentally invisible. Accordingly only a cis and a trans form, that have a sufficiently high barrier for their reciprocal interconversion, can be experimentally detected.

According to DFT calculations the *trans*-a conformer, where the dihedral angles for the *ortho*-nitrophenyl and for the *ortho*-tolyl are −154° and −144°, respectively, represents the global minimum of energy. The second most stable conformation corresponds to the *cis*-b conformer that has dihedral angles of −160° and +52°, respectively, and a 0.7 kcal/mol higher energy value (Table 1, second and third column).

Table 1
Dihedral angles and relative energies (kcal/mol) computed for the conformers of **1**

Conformer	Dihedral angles[a]	DFT[b]	DFT with solvent[c]	CCSD[d]
(*trans*-a)	−154,−144	0.0	0.0	1.5
(*cis*-b)	−160,+52	0.7	0.45	2.1
(*trans*-c)	−47,−62	2.7	1.9	0.6
(*cis*-d)	−44,+141	1.4	1.2	0.0

[a] The first and the second value correspond, respectively, to the dihedral angle between the plane of 2-nitrophenyl and of the tolyl with that of the heterocyclic ring.
[b] B3LYP/6-311++G(2d,p).
[c] PCM-B3LYP/6-311++G(2d,p).
[d] CCSD/6-31+G(d)//B3LYP/6-311++G(2d,p).

The trans to cis ratio theoretically predicted by this approach (according to the Boltzmann distribution it corresponds to 92:8 at −130 °C), does not match very well the almost equal proportion experimentally observed. Such a discrepancy might be due to an insufficient theoretical level of the calculations, or to the effects of the solvent.

To verify the former hypothesis the four stationary points (two trans and two cis) found by DFT were then recalculated as single point energy at the more accurate CCSD/6-31+G(d) level. The results actually modify the energy trend, and the best structures are now *cis*-d and *trans*-c, that are separated by 0.6 kcal/mol (fifth column of Table 1). On the other hand, when the solvent was considered in the DFT calculations (PCM model[13]) the energy difference is further reduced to 0.45 kcal/mol (fourth column of Table 1), with the *trans*-a, *cis*-b still the most stable forms.[14] On the basis the above results, the simpler DFT approach should be considered sufficiently reliable to tackle the conformation analysis of the present set of molecules because of its acceptable accuracy, coupled with a reasonable computational cost.[15]

The rotation barriers of the two rings (occurring through transition states where the aryl rings are almost coplanar with the nearly flat five-membered ring[16]) were DFT computed to be very close to each other (9.4 kcal/mol for the *ortho*-nitrophenyl and 8.9 kcal/mol for the *ortho*-tolyl), thus accounting for the impossibility of distinguishing the two experimental barriers: these values are also in reasonable agreement with observed value of 8.6 kcal/mol. No additional dynamic features were observed when the temperature was further lowered to −160 °C.

The enantiomerization barrier due solely to the rotation of the *ortho*-nitrophenyl ring can be observed in the case of compound **4**, where a phenyl has replaced the *ortho*-tolyl substituent: this is due to the fact that the rotational barrier of the unsubstituted phenyl is exceedingly low. As shown in Fig. S1 of Supplementary Data, the high-field signal of the CH_2 groups broadens and decoalesces below

−44 °C, showing two anisochronous signals due to the diastereotopicity of the hydrogens: the corresponding barrier was found to be 10.8 kcal/mol. This value is higher than that measured in compound **1** (8.6 kcal/mol), and indeed also the calculations predicted a value of 11.1 kcal/mol, which is also higher than that computed for the same rotational process in compound **1** (9.4 kcal/mol). The difference could be rationalized by considering that the ground state of compound **4** is more stabilized than that of **1**. In the ground state of **4** the phenyl ring can better conjugate with the five-membered unsaturated ring ($N_3{=}C_2{-}C_{ipso}{=}C_{ortho}$ dihedral angle 32° or −144°), a conjugation, that is, lost in the transition state where the phenyl is driven to be perpendicular by the rotation of the *ortho*-nitrophenyl ring. The stabilizing effect is smaller in the case of the tolyl group of compound **1** (dihedral angles 42° and −127°), thus the measured rotation barrier of the *ortho*-nitrophenyl is lower.

The near degeneracy of the two aryl rotation barriers observed in **1** was lifted in the case of the corresponding six-membered derivative **2**. The 600 MHz spectrum in $CDCl_3$ displays, in fact, sharp signals for all the hydrogens at +50 °C, whereas on cooling below ambient temperature, *only* the methylene multiplets begin to broaden and two of them eventually split into a pair of signals with equal intensity at −10 °C. This is most evident for the signal of the CH_2 in position 5 (at 2.19 ppm), which decoalesces below 25° to yield two equally intense multiplets (ABX_2Y_2 spin system) separated by 70 Hz at −10 °C (Fig. S2 of Supplementary Data): the corresponding barrier was determined to be 14.5 kcal/mol. As mentioned above this effect is a consequence of the restricted rotation of only one of the two aryl rings, which adopts a non-planar (thus chiral)[17] conformation making, consequently, diastereotopic *only* the methylene hydrogens.[18] This rotation process, in contrast, cannot affect neither the methyl nor any other signal of the molecule, as experimentally observed. It is impossible to ascertain solely on experimental ground whether it is the rotation of the *ortho*-nitrophenyl or that of the *ortho*-tolyl ring, which has been frozen. However the *ortho*-tolyl group experiences a less hindered environment with respect to the *o*-nitro phenyl, thus making the latter a more likely candidate for the observed process. DFT calculations indeed predict that the barrier for the *o*-nitro phenyl rotation should be 13.4 kcal/mol, definitely higher than that calculated for the *ortho*-tolyl (9.5 kcal/mol) and, in addition, much closer to the experimental value. Such a calculated difference explains why in compound **2** the two barriers can be distinguished, contrary to the case of **1**.

On further lowering the temperature (in $CDF_2Cl/CDFCl_2$) a second dynamic process involving all the signals is observed: in particular the single methyl line broadens and then splits at −80 °C into two lines, with a 70:30 ratio. This second process is due to the restriction of the *o*-tolyl ring rotation, which now generates, as in **1**, the trans and cis conformers: the experimental barrier is 10.7 kcal/mol, in reasonable agreement with the computed value (i.e., 9.5 kcal/mol). The fact that two different aryl rotation barriers were observed in **2** proves that the unique barrier observed in **1** was actually due to an accidental near coincidence of the barriers of the two aryl rotations.

When even lower temperatures are reached, a third dynamic process becomes visible. This was best followed by monitoring the methyl lines at the ^{13}C frequency since they are clearly isolated from the CH_2 carbon lines. Both the lines of the major trans and of the minor cis conformer broaden and then split into two at −130 °C: these four methyl lines are shown in Fig. 2. The barrier for this third process was estimated to be about 7 kcal/mol. The analogous process, observed in similar six-membered heterocyclic derivatives containing a double bond, had been assigned[7,8,19] to the restriction of the ring inversion process that have barriers of about 7 kcal/mol. DFT computations indicate that the two conformers (invertomers) arising from this motion (Scheme 2) actually correspond to theoretical minima: they were labeled *anti* or *syn*, depending as to whether the CH_2 in position 5 is *anti* or *syn* to the NO_2 group. As conceivable, the

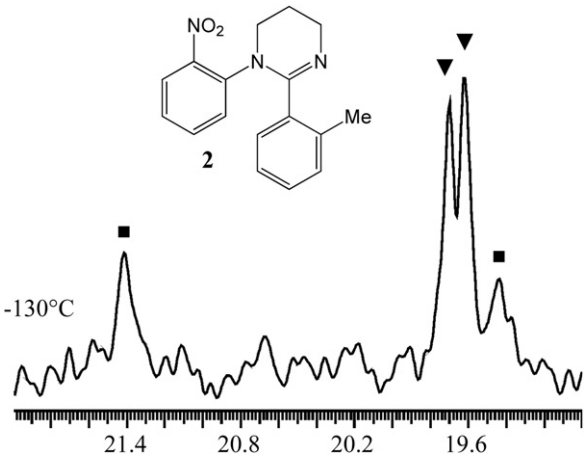

Fig. 2. ^{13}C methyl signals (150.8 MHz in $CDF_2Cl/CDFCl_2$) of compound **2** at low temperature showing that the major signal of the trans conformer is split into two lines (indicated by triangles) and likewise is split into two the signal of the minor cis conformer (indicated by squares).

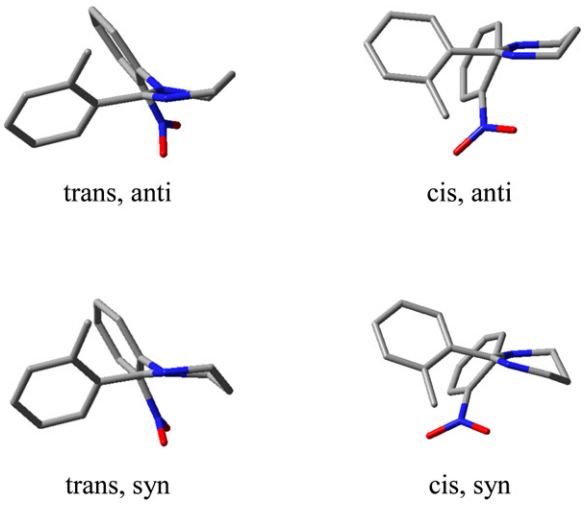

Scheme 2. DFT computed structures of the four conformers of compound **2** due to the restricted rotation of the two aryl rings (yielding cis and trans) and to the restricted inversion of the six-membered ring (yielding *syn* and *anti*).

experimental ratio of the two major is not equal to that of the two minor signals (Fig. 2), because they reflect the *anti* to *syn* ratio occurring in two different conformers (trans and cis).

The computed energy differences between the *anti* and *syn* invertomers are however quite high (1.3 and 2.2 kcal/mol, in the case of the conformer trans and cis, respectively) and do not agree with the nearly equal proportion experimentally observed in Fig. 2. Again this feature is likely to be a consequence of the insufficient accuracy of the level of computation or to the solvent effects, as mentioned above: being **2** an even larger molecule than **1**, more accurate computations were, unfortunately, outside the capability of our computation facilities.[13]

In the case of the seven-membered derivative **3** the dynamic effect is observed simultaneously on the methyl as well as on the methylene lines, indicating, that the rotation of the *ortho*-nitrophenyl and *ortho*-tolyl rings take place almost simultaneously and cannot be distinguished, as already observed in compound **1**. The ratio of the two rotational conformers, as detected by ^{13}C at −140 °C, is about 70:30. Only two lines were visible, indicating that only the two conformers trans and cis are present, in that the conformational effects of ring inversion were not observed. This is quite reasonable since the rate of the ring inversion process is

expected to be very fast in a seven-membered ring and to escape NMR observation, even at quite low temperature.[20] The complexity of the spectrum of compound **3** also prevented the determination of the experimental barrier for the cis/trans interconversion. Since such a process occurs, however, in the same temperature range as that of **1**, it is conceivable to expect a similar value for the interconversion barrier.

3. Conclusion

The restricted rotation of aryl rings linked to five-, six-, and seven-membered heterocyclic rings were detected by Dynamic NMR and computed by DFT calculations. In the case of the six-membered tetrahydropyrimidine ring the additional conformers resulting from a ring inversion process were also detected.

4. Experimental

4.1. General

Melting points were determined with a Büchi capillary apparatus and are uncorrected. IR spectra were recorded on a Perkin–Elmer Spectrum One FT-IR spectrometer. ^{1}H NMR spectra were recorded on a Bruker Avance II 500 MHz spectrometer, using deuteriochloroform as the solvent. Chemical shifts are reported in parts per million (δ) relative to TMS as an internal standard. D_2O was employed to confirm exchangeable protons (ex). Splitting multiplicities are reported as singlet (s), broad signal (br s), doublet (d), double doublet (dd), doublet of double doublets (ddd), triplet (t), double triplet (dt), quartet (q), pentet (p), and multiplet (m). HRMS (ESI) were performed with a Bruker MicroTOF-Q II spectrometer. Reagents, solvents, and starting materials were purchased from standard sources and purified according to literature procedures.

4.2. Synthesis of compounds 1–4

Amidines **1**–**4** were synthesized by microwave-assisted ring closure of the corresponding *N*-acyl-*N′*-aryl-1,*n*-diamines.[21,22] Reactions were performed in a 1 mmol scale. Compound **4** was already described in the literature.[23] Yields and physical data of new compounds are as follows.

4.2.1. 1-(2-Nitrophenyl)-2-(2-methylphenyl)-imidazoline ***1***. This compound was obtained as a yellow solid (222.0 mg, 79%), mp 116–118 °C (chloroform/hexane). ν_{max} (KBr) 3006, 2989, 1621, 1524, 1487, 1347, 1275, 1138, 1090, 851, 706 cm^{-1}. ^{1}H NMR (500 MHz, $CDCl_3$, 25 °C, TMS): δ=7.75 (1H, dd, *J*=8.1, 1.4 Hz), 7.36–7.42 (1H, m), 7.19–7.26 (2H, m), 7.15–7.19 (1H, m), 7.12 (1H, dt, *J*=7.6, 0.7 Hz), 7.03–7.09 (2H, m), 4.18–4.23 (2H, m), 3.95–4.01 (2H, m), 2.37 (3H, s). ^{13}C NMR (125 MHz, $CDCl_3$, 25 °C): δ=162.1, 144.7, 137.4, 136.6, 133.2, 130.8, 129.6, 129.6, 129.4, 127.8, 125.6, 125.4, 125.3, 54.6, 52.7, 19.9. HRMS (ESI) MH$^+$, found 282.1248. $C_{16}H_{16}N_3O_2$ requires 282.1242.

4.2.2. 1-(2-Nitrophenyl)-2-(2-methylphenyl)-1,4,5,6-tetrahydropyrimidine ***2***. This compound was obtained as a yellow solid (268.4 mg, 91%), mp 115–116 °C (chloroform/hexane). ν_{max} (KBr) 2853, 2099, 1634, 1523, 1483, 1349, 1301, 1217, 1090, 852, 766, 705 cm^{-1}. ^{1}H NMR (500 MHz, $CDCl_3$, 25 °C, TMS): δ=7.75 (1H, dd, *J*=8.1, 1.5 Hz), 7.41–7.45 (1H, m), 7.25 (1H, d, *J*=7.8 Hz), 7.17–7.21 (1H, m), 7.05–7.08 (1H, m), 7.03 (1H, dd, *J*=7.6, 1.4 Hz), 6.96–6.99 (1H, m), 6.90–6.94 (1H, m), 3.79 (2H, br s), 3.74 (2H, t, *J*=5.5 Hz), 2.35 (3H, s), 2.19 (2H, br s). ^{13}C NMR (125 MHz, $CDCl_3$, 25 °C): δ=154.7, 139.8, 135.7 (br s), 133.4, 130.3, 128.7, 128.5, 126.8 (br s), 125.4 (br s), 125.4, 50.0, 44.7, 21.7, 19.4. HRMS (ESI) MH$^+$, found 296.1403. $C_{17}H_{18}N_3O_2$ requires 296.1399.

4.2.3. 1-(2-Nitrophenyl)-2-(2-methylphenyl)-1,4,5,6-tetrahydrodiazepine ***3***. This compound was obtained as a yellow solid (278.1 mg, 90%), mp 98–99 °C (chloroform/hexane). ν_{max} (KBr) 2859, 2099, 1636, 1522, 1482, 1347, 1295, 1154, 1049, 852, 768, 707 cm^{-1}. ^{1}H NMR (500 MHz, $CDCl_3$, 25 °C, TMS): δ=7.69 (1H, dd, *J*=8.2, 1.6 Hz), 7.40–7.45 (1H, m), 7.33 (1H, dd, *J*=8.2, 1.3 Hz), 7.15 (1H, dd, *J*=7.7, 1.3 Hz), 7.02–7.10 (2H, m), 6.91–6.99 (2H, m), 4.00–4.05 (2H, m), 3.93–3.98 (2H, m), 2.37 (3H, s), 2.08–2.16 (2H, m), 2.02 (2H, p, *J*=6.1 Hz). ^{13}C NMR (125 MHz, $CDCl_3$, 25 °C): δ=157.6, 144.9, 140.3, 136.7, 136.4, 133.2, 130.5, 129.7, 128.9, 126.9, 125.8, 125.4, 124.8, 52.5, 49.0, 26.1, 24.8, 19.8. HRMS (ESI) MH$^+$, found 310.1559. $C_{18}H_{20}N_3O_2$ requires 310.1556.

N-(2-Methylbenzoyl)-*N′*-(2-nitrophenyl)-1,*n*-diamines were synthesized by selective monoacylation of the corresponding *N*-(2-nitrophenyl)-1,*n*-diamines. *N*-benzoyl-*N′*-(2-nitrophenyl)-1,2-ethanediamine was described in the literature.[23] Reactions were performed in a 1 mmol scale. Yields and physical data of new compounds are as follows.

4.2.4. N-(2-Methylbenzoyl)-N′-(2-nitrophenyl)-1,2-ethanediamine. This compound was obtained as a yellow solid (218.3 mg, 73%), mp 82–83 °C (chloroform/hexane). ν_{max} (KBr) 3435, 2103, 1641, 1573, 1511, 1418, 1353, 1320, 1262, 1231, 1157, 1037, 741 cm^{-1}. ^{1}H NMR (500 MHz, $CDCl_3$, 25 °C, TMS): δ=8.23 (1H, br s ex), 8.18 (1H, dd, *J*=8.5, 1.5 Hz), 7.48 (1H, ddd, *J*=8.5, 7.0, 1.1 Hz), 7.29–7.37 (2H, m), 7.16–7.25 (2H, m), 7.03 (1H, dd, *J*=8.5, 0.8 Hz), 6.70 (1H, ddd, *J*=8.5, 7.1, 1.1 Hz), 6.29 (1H, br s ex), 3.74 (2H, q, *J*=6.0 Hz), 3.64 (2H, q, *J*=6.0 Hz), 2.45 (3H, s). ^{13}C NMR (125 MHz, $CDCl_3$, 25 °C): δ=170.7, 145.3, 136.5, 136.2, 135.7, 131.2, 131.1, 130.2, 127.0, 126.7, 125.8, 115.9, 113.7, 42.3, 39.1, 19.8. HRMS (ESI) MNa$^+$, found 322.1171. $C_{16}H_{17}N_3NaO_3$ requires 322.1168.

4.2.5. N-(2-Methylbenzoyl)-N′-(2-nitrophenyl)-1,3-propanediamine. This compound was obtained as a yellow solid (256.7 mg, 82%), mp 105–106 °C (chloroform/hexane). ν_{max} (KBr) 3435, 2102, 1641, 1573, 1512, 1440, 1418, 1354, 1309, 1268, 1232, 1154, 1037, 741 cm^{-1}. ^{1}H NMR (500 MHz, $CDCl_3$, 25 °C, TMS): δ=8.19 (1H, dd, *J*=8.5, 1.5 Hz), 8.13 (1H, br s ex), 7.44–7.49 (1H, m), 7.30–7.37 (2H, m), 7.18–7.26 (2H, m), 6.89 (1H, dd, *J*=8.70, 0.9 Hz), 6.68 (1H, ddd, *J*=8.5, 7.0, 1.1 Hz), 6.04 (1H, br s ex), 3.61 (2H, q, *J*=6.9 Hz), 3.47 (2H, td, *J*=6.9, 5.6 Hz), 2.46 (3H, s), 2.07 (2H, p, 6.9). ^{13}C NMR (125 MHz, $CDCl_3$, 25 °C): δ=170.4, 145.3, 136.3, 136.2, 136.0, 132.1, 131.1, 130.0, 127.0, 126.58, 125.8, 115.5, 113.6, 40.7, 37.5, 29.4, 19.8. HRMS (ESI) MNa$^+$, found 336.1330. $C_{17}H_{19}N_3NaO_3$ requires 336.1324.

4.2.6. N -(2-Methylbenzoyl)-N′-(2-nitrophenyl)-1,4-butanediamine. This compound was obtained as a yellow solid (209.3 mg, 64%), mp 94–95 °C (chloroform/hexane). ν_{max} (KBr) 3383, 2096, 1637, 1573, 1473, 1440, 1418, 1379, 1354, 1308, 1232, 1153, 1037, 777 cm^{-1}. ^{1}H NMR (500 MHz, $CDCl_3$, 25 °C): δ=8.18 (1H, dd, *J*=8.7, 1.6 Hz), 8.08 (1H, br s ex), 7.42–7.48 (1H, m), 7.30–7.37 (2H, m), 7.17–7.25 (2H, m), 6.88 (1H, dd, *J*=8.5, 0.8 Hz), 6.67 (1H, ddd, *J*=8.5, 7.0, 1.1 Hz), 5.94 (1H, br s ex), 3.52 (2H, q, *J*=6.6 Hz), 3.36–3.44 (2H, m), 1.74–1.90 (4H, m), 2.45 (3H, s). ^{13}C NMR (125 MHz, $CDCl_3$, 25 °C, TMS): δ=170.3, 145.4, 136.4, 136.3, 136.0, 131.9, 131.0, 129.88, 126.9, 126.6, 125.7, 115.3, 113.7, 42.5, 39.2, 27.4, 26.4, 19.8. HRMS (ESI) MNa$^+$, found 350.1483. $C_{18}H_{21}N_3NaO_3$ requires 350.1481.

4.3. Variable temperature NMR spectroscopy

NMR spectra were recorded using a Varian INOVA spectrometer operating at a field of 14.4 T (600 MHz for ^{1}H and 150.8 for ^{13}C). The

NMR tubes containing the compounds were linked to a vacuum line, immersed in liquid nitrogen and evacuated in order to condense about 0.6 ml of a mixture of gaseous $CDFCl_2/CDF_2Cl$ obtained by reacting $CDCl_3$ with SbF_3 and SbF_5 as described in the literature.[24] The tubes were subsequently sealed under reduced pressure (0.01 mbar) using a methane/oxygen torch. The samples were cautiously warmed to +25 °C, where the solvent develops a pressure of about 8 atm. After a few hours at ambient temperature, the samples could be safely introduced into the probe head of the spectrometer, already cooled to −30 °C. Low temperature 600 MHz ^{1}H spectra were acquired without spinning using a 5 mm dual direct probe with a 9000 Hz sweep width, 2.0 μs (20° tip angle) pulse width, 3 s acquisition time, and 1 s delay time. A shifted sine bell weighting function[25] equal to the acquisition time (i.e., 3 s) was applied before the Fourier transformation. Low temperature 150.8 MHz ^{13}C spectra were acquired without spinning and under proton decoupling conditions with a 38,000 Hz sweep width, 4.2 μs (60° tip angle) pulse width, 1 s acquisition time, and 1 s delay time. A line broadening function of 1–2 Hz was applied before the Fourier transformation. To reach the required low temperature a flow of dry nitrogen was first passed through a pre-cooling unit adjusted to −50 °C. The gas entered into an inox steel heat-exchanger immersed in liquid nitrogen and connected to the NMR probe head by a vacuum-insulated transfer line. Gas flows of 10–40 L min^{-1} were required to descend to the desired temperature. Temperature calibrations were performed before the experiments, using a digital thermometer and a Cu/Ni thermocouple placed in an NMR tube filled with isopentane. The conditions were kept as equal as possible with all subsequent work. In particular, the sample was not spun and the gas flow was the same as that used during the acquisition of the spectra. The uncertainty in temperature measurements can be estimated as ±2 °C.

Line shape simulations were performed using a PC version of the QCPE DNMR6 program.[26] Electronic superimposition of the original spectrum and of the simulated one enabled the determination of the most reliable rate constant.

4.4. Calculations

Geometry optimization were carried out at the B3LYP/6-31G(d) level by means of the Gaussian 09 series of programs[27] The standard Berny algorithm in redundant internal coordinates and default criteria of convergence were employed. The harmonic vibrational frequencies were calculated for all the stationary points. For each optimized ground state the frequency analysis showed the absence of imaginary frequencies, whereas each transition state showed a single imaginary frequency. Visual inspection of the corresponding normal mode was used to confirm that the correct transition state had been found. If not explicitly indicated, the reported energy values represent the total electronic energies. In general, these give the best fit with experimental Dynamic-NMR data.[26b,28] This approach avoids artifacts that might result from the ambiguous choice of the adequate reference temperature, and from the idealization of low-frequency vibrators as harmonic oscillators (very important in the present cases, where about one third of the calculated frequencies fall below the 500–600 cm^{-1} range).

Acknowledgements

Financial contribution (to L.L and A.M.) was received from the University of Bologna (RFO) and from MIUR, Rome (PRIN national project 'Stereoselection in Organic Synthesis, Methodologies, and Applications'). Support (to L.R.O.) was also obtained from Universidad de Buenos Aires and CONICET

Supplementary data

Supplementary data associated with this article can be found, in the online version, at doi:10.1016/j.tet.2011.09.091.

References and notes

1. Dunbar, P. G.; Durant, G. J.; Fang, Z. *J. Med. Chem.* **1993**, *36*, 842–847.
2. Dunbar, P. G.; Durant, G. J.; Rho, T. *J. Med. Chem.* **1994**, *37*, 2774–2782.
3. Bernard, T.; Jebbar, M.; Rassouli, Y.; Himdi-Kabbab, S.; Hamelin, J.; Blanco, C. *J. Gen. Microbiol.* **1993**, *139*, 129–136.
4. Weinhardt, K.; Wallach, M. B.; March, M. *J. Med. Chem.* **1985**, *28*, 694–698.
5. Carter, P.A.; Pfrendle, W.F. UK Patent Appl. GB 2,277,090, 1994; *Chem. Abstr.* **1994**, *122*, 31544b.
6. McFarland, J. W.; Howes, H. L. *J. Med. Chem.* **1972**, *15*, 365–368.
7. Garcia, M. B.; Grilli, S.; Lunazzi, L.; Mazzanti, A.; Orelli, L. R. *J. Org. Chem.* **2001**, *66*, 6679–6684.
8. Garcia, M. B.; Grilli, S.; Lunazzi, L.; Mazzanti, A.; Orelli, L. R. *Eur. J. Org. Chem.* **2002**, 4018–4023.
9. The fact that the ratio of these two lines is different from 1:1 is proved by the observation that the two lines have a 58:42 intensity in a Me_2O solution at the same temperature.
10. Eyring, H. *Chem. Rev.* **1935**, *17*, 65–77.
11. (a) Lunazzi, L.; Mancinelli, M.; Mazzanti, A. *J. Org. Chem.* **2007**, *72*, 5391–5394; (b) Casarini, D.; Lunazzi, L.; Mazzanti, A. *Eur. J. Org. Chem.* **2010**, *75*, 2035–2056.
12. (a) Anderson, J. E.; Casarini, D.; Lunazzi, L. *Tetrahedron Lett.* **1988**, *29*, 3141–3144; (b) Lunazzi, L.; Mancinelli, M.; Mazzanti, A. *J. Org. Chem.* **2007**, *72*, 10045–10050.
13. For a review see: Tomasi, J.; Mennucci, B.; Cammi, R. *Chem. Rev.* **2005**, *105*, 2999–3093 (the calculations were performed by setting $CHCl_3$ as the solvent, because its parameters are the most similar to those of $CDFCl_2$).
14. CCSD calculations including the solvent are behind our computing facilities.
15. A single point CCSD/6-31+G(d) calculation on compound **1** takes about one week on an 8-cores job running on Xeon X7355 processors @ 2.93 GHz, with a scratch file of about 120 Gbytes. CCSD calculations scale roughly with N^6 (N being the number of the basis functions, i.e., of the orbitals), so this approach would require computational times close to a month when dealing with larger molecules like compounds **2** and **3**. On the other hand, an optimization with DFT and the subsequent frequency calculation usually takes 8–16 h.
16. There are actually two possible transition states for the rotation of each aryl ring, the threshold transition states correspond to the passage of the nitro group across the CH_2 in position 5, and to the passage of the *ortho*-methyl group across the nitrogen in position 3. The alternative transition states have much higher energies and therefore are not feasible.
17. As discussed in the case of **1** the frozen aryl ring adopts a conformation where its plane is not coplanar with respect to the dynamic plane of the six-membered ring, which undergoes a rapid ring inversion at this temperature.
18. (a) Mislow, K.; Raban, M. *Top. Stereochem.* **1967**, *1*, 1–38; (b) Jennings, W. B. *Chem. Rev.* **1975**, *75*, 307–322; (c) Eliel, E. L. *J. Chem. Educ.* **1980**, *57*, 52–55; (d) Casarini, D.; Lunazzi, L.; Macciantelli, D. *J. Chem. Soc., Perkin Trans. 2* **1992**, 1363–1370.
19. (a) Oki, M. *Applications of Dynamic NMR Spectroscopy to Organic Chemistry*; VCH: Deerfield Beach, Florida, 1985; 306; (b) Kleinpeter, E. In *Advances in Heterocyclic Chemistry*; Katritzky, A. R., Ed.; Elsevier: 2004; Vol. 86, 109.
20. In principle it cannot be excluded that the ring inversion process had been frozen but only one of the resulting conformers (invertomers) is populated. This occurrence would also be compatible with the absence of observable NMR dynamic effects.
21. García, M. B.; Torres, R. A.; Orelli, L. R. *Tetrahedron Lett.* **2006**, *47*, 4857–4859.
22. Díaz, J. E.; Bisceglia, J. A.; Mollo, M. C.; Orelli, L. R. *Tetrahedron Lett.* **2011**, *52*, 1895–1897.
23. Perillo, I. A.; Lamdan, S. *J. Heterocycl. Chem.* **1970**, *7*, 791–798.
24. Siegel, J. S.; Anet, F. A. L. *J. Org. Chem.* **1988**, *53*, 2629–2630.
25. Claridge, T. D. W. *High-resolution NMR Techniques in Organic Chemistry*; Pergamon: Oxford, 1999; 71.
26. (a) Brown, J. H.; Bushweller, C. H. *DNMR6: (program 633) QCPE Bulletin*; Bloomington: Indiana, 1983; Vol. 3; 103–103; (b) A copy of the program is available on request from the authors (L. L. and A. M.).
27. Frisch, M. J.; Trucks, G. W.; Schlegel, H. B.; Scuseria, G. E.; Robb, M. A.; Cheeseman, J. R.; Scalmani, G.; Barone, V.; Mennucci, B.; Petersson, G. A.; Nakatsuji, H.; Caricato, M.; Li, X.; Hratchian, H. P.; Izmaylov, A. F.; Bloino, J.; Zheng, G.; Sonnenberg, J. L.; Hada, M.; Ehara, M.; Toyota, K.; Fukuda, R.; Hasegawa, J.; Ishida, M.; Nakajima, T.; Honda, Y.; Kitao, O.; Nakai, H.; Vreven, T.; Montgomery, J. A., Jr.; Peralta, J. E.; Ogliaro, F.; Bearpark, M.; Heyd, J. J.; Brothers, E.; Kudin, K. N.; Staroverov, V. N.; Kobayashi, R.; Normand, J.; Raghavachari, K.; Rendell, A.; Burant, J. C.; Iyengar, S. S.; Tomasi, J.; Cossi, M.; Rega, N.; Millam, N. J.; Klene, M.; Knox, J. E.; Cross, J. B.; Bakken, V.; Adamo, C.; Jaramillo, J.; Gomperts, R.; Stratmann, R. E.; Yazyev, O.; Austin, A. J.; Cammi, R.; Pomelli, C.; Ochterski, J. W.; Martin, R. L.; Morokuma, K.; Zakrzewski, V. G.; Voth, G. A.; Salvador, P.; Dannenberg, J. J.; Dapprich, S.; Daniels, A. D.; Farkas, Ö; Foresman, J. B.; Ortiz, J. V.; Cioslowski, J.; Fox, D. J. *Gaussian 09, Revision A.02*; Gaussian: Wallingford CT, 2009.
28. Ayala, P. Y.; Schlegel, H. B. *J. Chem. Phys.* **1998**, *108*, 2314–2325.